γ-ray spectroscopy in 111Te

著者	Starosta K., Chiara C. J., Fossan D. B., Koike T., LaFosse D. R., Lane G. J., Sears J. M., Smith J. F., Boston A. J., Nolan P. J., Paul E. S., Semple A. T., Devlin M., Sarantites D. G., Lee I. Y., Macchiavelli A. O.
journal or publication title	Physical Review. C
volume	61
number	3
page range	034308
year	2000
URL	http://hdl.handle.net/10097/52596

doi: 10.1103/PhysRevC.61.034308

γ-ray spectroscopy in ^{111}Te

K. Starosta,* C. J. Chiara, D. B. Fossan, T. Koike, D. R. LaFosse, G. J. Lane,† J. M. Sears, and J. F. Smith‡
Department of Physics and Astronomy, State University of New York at Stony Brook, Stony Brook, New York 11794-3800

A. J. Boston, P. J. Nolan, E. S. Paul, and A. T. Semple
Oliver Lodge Laboratory, University of Liverpool, Liverpool L69 7ZE, United Kingdom

M. Devlin§ and D. G. Sarantites
Department of Chemistry, Washington University, St. Louis, Missouri 63130

I. Y. Lee and A. O. Macchiavelli
Nuclear Science Division, Lawrence Berkeley National Laboratory, Berkeley, California 94720
(Received 19 October 1999; published 17 February 2000)

Excited states in ^{111}Te have been studied using the $4pn$ evaporation channel from the ^{58}Ni+^{58}Ni reaction at a beam energy of 250 MeV. A thin-target experiment was carried out using GAMMASPHERE coupled with the MICROBALL charged-particle detector array and an array of neutron detectors. A complementary thick-target experiment was performed with the Stony Brook six-Ge-detector array in order to measure the lifetime of an $11/2^-$ isomer observed in the GAMMASPHERE data. The structure of ^{111}Te at low spin is dominated by the yrast $\nu h_{11/2}$ band, although a band assigned to the $\nu(g_{7/2}d_{5/2})$ configuration is also observed. Four collective bands have been found at higher spins. Experimental results are compared to the odd-A Te systematics and to core-quasiparticle and total Routhian surface calculations.

PACS number(s): 21.10.Re, 21.10.Tg, 23.20.Lv, 27.60+j

I. INTRODUCTION

In the present paper the experimental results extracted for ^{111}Te, which extend the systematics of low-spin states in odd-A Te nuclei, are presented. Comparisons of the observed energy levels to those calculated using theoretical models allow the investigation of the properties of the low-spin collective states together with those in neighboring even-A Te nuclei. Even-A Te isotopes at low spin are usually considered to be vibrational, as indicated by the energy ratios for low-lying states, $E(4^+)/E(2^+)\approx 2$. One of the features of surface harmonic vibration is a small value for the diagonal matrix element of the $E2$ operator, which implies correspondingly small quadrupole moments. However, core-quasiparticle coupling calculations with a quadrupole-quadrupole interaction performed for the negative-parity states in ^{111}Te indicate a significant spectroscopic quadrupole moment for the Te core. These contradictory issues will be discussed. The core may be deformed due to the deformation-driving force exerted by the valence $h_{11/2}$ neutron, although a possible quadrupole deformation at low spin for the even-A Te with $A\sim 110$ cannot be excluded. Sizable spectroscopic quadrupole moments have indeed been measured for heavier even-A Te isotopes [1].

II. EXPERIMENTAL METHOD

Excited states in ^{111}Te were populated following the ^{58}Ni(^{58}Ni,$4pn$) reaction at a beam energy of 250 MeV. The experimental setup consisted of the GAMMASPHERE array of 83 HPGe detectors coupled with the MICROBALL array of 95 CsI(Tl) charged-particle detectors [2], and an array of 15 scintillators for neutron detection which replaced the 15 front Ge detectors. Two self-supporting ~ 500 μg/cm^2 stacked targets separated by a distance of ~ 0.25 mm were used. The average velocity of the recoiling nuclei was measured to be $\beta\sim 4.4\%$ in agreement with the value calculated based on reaction kinematics. Measured γ-ray energies were corrected off line for Doppler shifts. The Doppler correction procedure involved event-by-event reconstruction of the momentum vector of the residual nucleus based on reaction kinematics and measured charged-particle momentum vectors [2]. In the $4pn$ channel, a γ-ray energy resolution of 5.5 keV full width at half maximum (FWHM) at 1 MeV was achieved with this procedure.

For the off-line analysis, coincident γ-ray events were sorted into a $4pn$-gated E_γ-E_γ matrix, $4p$-, $3p$-, and $3pn$-gated cubes, and $4p$- and $3p$-gated hypercubes. Applied proton and neutron gates turned out to be essential to achieve the sensitivity required for γ-ray spectroscopic studies of weakly populated ^{111}Te. In the $4p$-gated data, the $4pn$ evaporation channel had an intensity of $\sim 2.4\%$ compared to the intensity of the $4p$ evaporation channel which leads to ^{112}Te, while in the $3pn$-gated data, the $4pn$ evaporation channel had an intensity of $\sim 30\%$ compared to the $3pn$ evaporation channel which leads to ^{112}I. In the $4pn$-gated

*On leave from Institute of Experimental Physics, Warsaw University, Hoża 69, 00-681 Warsaw, Poland.

†Present address: Nuclear Science Division, Lawrence Berkeley National Laboratory, Berkeley, CA 94720.

‡Present address: Schuster Laboratory, The University of Manchester, Manchester M13 9PL U.K.

§Present address: LANSCE-3, Los Alamos National Laboratory, Los Alamos, NM 87545.

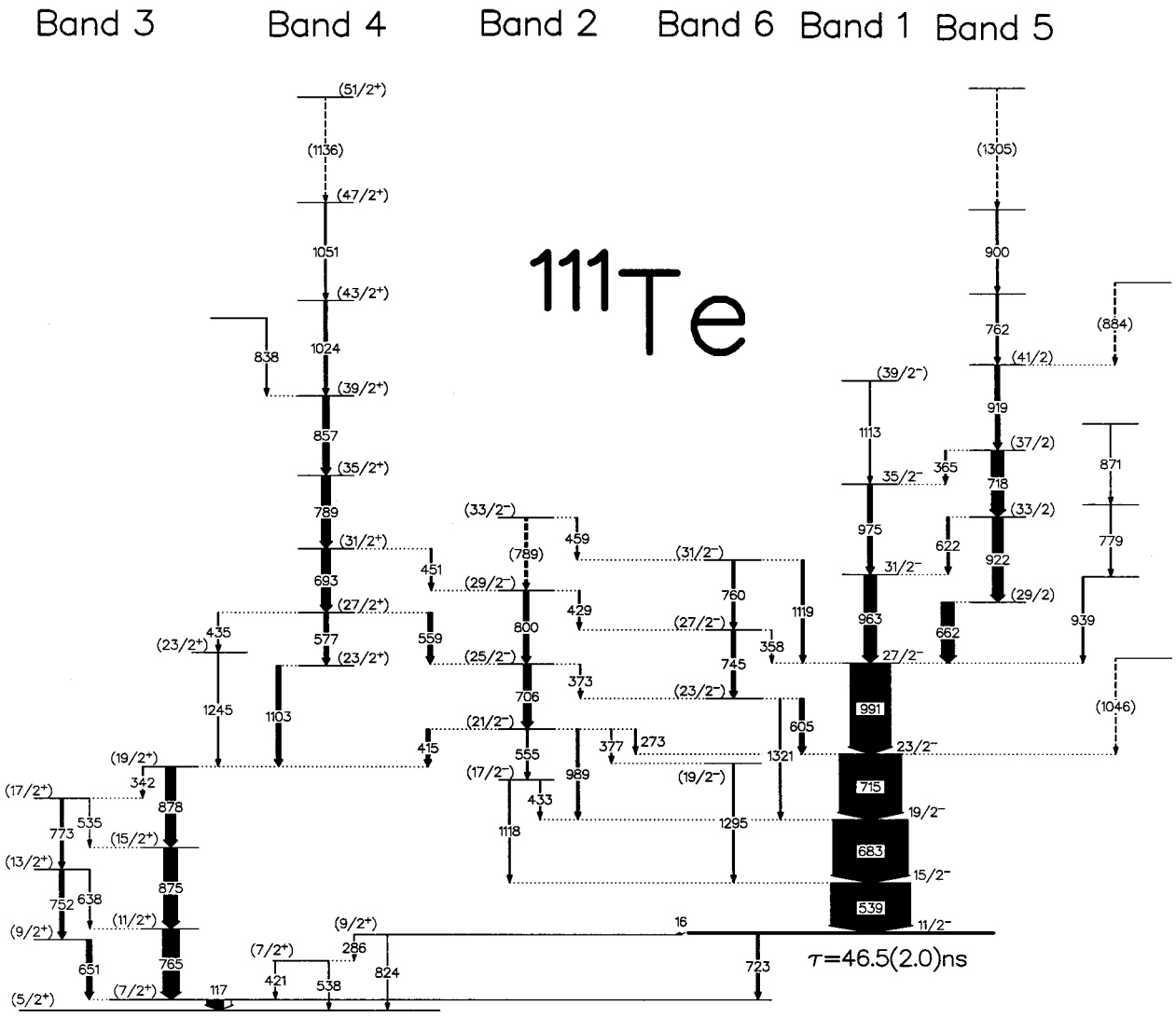

FIG. 1. Proposed level scheme for ^{111}Te. The width of the arrows represents the relative intensity of the γ-ray transitions.

matrix containing 4.1×10^6 counts the intensity of ^{111}Te was $\sim$82%. The γ-ray spectroscopy software package RADWARE [3] was used extensively during the data analysis.

An angular correlation (DCO) study [4] was performed for γ-ray multipolarity assignments. Asymmetric DCO $4pn$-, $3pn$-, and $3p$-gated matrices were sorted with data from the detectors at $\theta>142\,^\circ$ incremented on one axis and from the detectors at $79\,^\circ<\theta<101\,^\circ$ on the other axis (note that the forward rings of Ge detectors were replaced by neutron detectors). The number of counts in the $4pn$- and $3pn$-gated DCO matrices were 0.7×10^6 and 2×10^6, respectively. DCO ratios [4] extracted from the $3p$-gated matrix for known quadrupole-dipole and quadrupole-quadrupole cascades in ^{113}I [5] are $R_{\rm DCO}=0.65(3)$ for the $15/2^-\rightarrow11/2^-\rightarrow9/2^+$ cascade and $R_{\rm DCO}=0.99(5)$ for the $19/2^-\rightarrow15/2^-\rightarrow11/2^-$ cascade.

Analysis of the γ-ray intensities measured in the thin-target GAMMASPHERE experiment suggested that the $11/2^-$ bandhead of the yrast band is an isomer. To determine its lifetime, an experiment with the same reaction but a thick target ($\sim$2 mg/cm^2 ^{58}Ni on a Pb backing) was performed using the tandem van de Graaff/superconducting LINAC facility and six Ge-detector array of the Nuclear Structure Laboratory at Stony Brook. Two beam sweeping periods of 106 ns and 318 ns were employed. The Compton-suppressed Ge detectors were placed at approximately $\pm30\,^\circ$, $90\,^\circ$, and $\pm150\,^\circ$ with respect to the beam axis.

III. EXPERIMENTAL RESULTS

Excited states in ^{111}Te had been assigned previously in Ref. [6] through prompt-prompt γ-γ and γ-neutron and prompt-delayed γ-recoil coincidence techniques. In this previous experiment, the yrast band was observed and several other transitions were identified as belonging to ^{111}Te. The current study extends the level scheme significantly. It also confirms the previous channel assignment via charged-particle and neutron coincidences.

The level scheme proposed for ^{111}Te is presented in Fig. 1. Energies, intensities, DCO ratios, proposed multipo-

larities of the γ-ray transitions, and spin assignments for excited levels in ^{111}Te are listed in Tables I and II. The quality of the GAMMASPHERE and MICROBALL data is illustrated in Fig. 2, which presents $4pn$-gated γ-γ coincidence spectra gated on the 963- and 1103-keV transitions. The details of γ-ray placement in the level scheme, level spin assignments, and comparisons with Ref. [6] are summarized below.

A. Negative-parity bands and band 5

Band 1 is yrast between spins $11/2\hbar$ and $35/2\hbar$. The ordering of the 683- and 715-keV transitions proposed in the current study is reversed compared to that in Ref. [6] where arguments based on odd-*A* Te systematics were used. In the present study, the ordering of these transitions is fixed by the observed decay of the $(21/2^-)$ level in band 2 and the $(23/2^-)$ level in band 6. Other differences between the current level scheme and that proposed in Ref. [6] occur at high spin. A coincidence between the 922- and 963-keV transitions suggested in Ref. [6] was not confirmed (see upper panel of Fig. 2). In the current study, self-coincidence between transitions with energy $\sim$920 keV was observed, indicating the existence of a doublet at 919 and 922 keV in coincidence with the yrast transitions. These data suggest that the 922-keV transition does not belong to the yrast cascade, but rather to band 5, while the 919-keV transition belongs to the same band and is connected via 365- and 622-keV γ rays to the yrast states, which explains the weak 963-919-keV coincidence. The 622-, 762-, and 789-keV transitions assigned tentatively to ^{111}Te in Ref. [6] were observed in this work; the 622-keV transition was observed connecting the (33/2) state in band 5 to the $31/2^-$ state in band 1, and the 762-keV and 789-keV transitions were observed as intraband transitions in bands 5 and 4, respectively.

The spin assignments for the states belonging to band 1 follow from the observed DCO ratios (all transitions below $35/2^-$ have $R_{\rm DCO}$ consistent with stretched $E2$) and from odd-*A* Te systematics. The systematics includes excitation energies of collective yrast states (see Sec. IV B) as well as the excitation energy and lifetime of the isomeric yrast bandhead (see discussion in Sec. IV G).

The DCO ratio measured for the 745-keV transition in band 6 suggests a stretched $E2$ character; the same is proposed for the 760-keV band member. If band 6 has positive parity, the 605-, 1119-, and 1321-keV transitions linking the band to the yrast states ought to be $|\Delta I|=1$ $E1$ transitions. The DCO ratio measured for the 605-keV transition contradicts this hypothesis. Therefore, negative parity is proposed for band 6 with an $I_i=I_f$ $M1/E2$ assignment for the 605-keV γ ray, which is then consistent with experimental $R_{\rm DCO}$. A stretched $E2$ character for both the 1119-keV and 1321-keV transitions is a consequence of this proposed spin assignment.

Band 2 decays to the the negative-parity states in bands 1 and 6. The DCO ratios measured for the 273- and 429-keV γ rays are consistent with a stretched dipole assignment, although the $M1$ or $E1$ character of those transitions cannot be determined in the current experiment. The spins and parity proposed for the states in band 2 in Fig. 1 follow from a comparison to the negative-parity states observed in Ref. [7] for ^{109}Te and the systematics of odd-*A* Te isotopes (see Sec. IV B).

The DCO ratios observed for the interband transitions between bands 1 and 5 are consistent with a stretched dipole character. A band in ^{109}Te which is similar to band 5 in ^{111}Te was assigned negative parity in Ref. [8], but was tentatively assigned to have positive parity in Refs. [7,9]. In all three studies the parity assignment was based on angular correlation measurements only. In Fig. 1 we have given only spins for band 5; the parity requires a polarization experiment designed to determine the electric or magnetic character of the transitions depopulating the band (see Sec. IV E).

For unresolved doublets at 715 and 718 keV and at 919 and 922 keV the effective value of the DCO ratio (which is the ratio of the summed intensities of both transitions) was measured. DCO ratios for the 715-718- and the 919-922-keV pairs are consistent with each transition being stretched quadrupole, although for the excited states in band 5, tentative spins are given only up to (41/2) since the current data are not adequate for assignments to states higher in excitation energy.

B. Positive-parity bands

The present ordering of the transitions in bands 3 and 4 follows from observed coincidence and intensity relationships (for example see lower panel of Fig. 2). Transitions with energies 117, 765, and a doublet at 875 and 878 keV in band 3 and 577, 693, 789, and 857 keV in band 4 were assigned to ^{111}Te in the experiment reported in Ref. [6] but were not placed in the level scheme, due to limited statistics.

The relative spins assigned to the excited states in bands 3 and 4 follow from stretched quadrupole assignments for the 765-keV transition, and the doublet at 875 and 878 keV in band 3, the 693-, 789-, and 857-keV transitions in band 4, and the 577- and 1103-keV transitions which connect bands 3 and 4. The absolute spin values for these states are proposed on the basis of the multipolarity assignments for the transitions connecting bands 3 and 4 to band 2. The 559-keV transition connecting bands 4 and 2 has a DCO ratio consistent with a stretched dipole. The same is true for the 415-keV transition connecting band 2 to 3. A DCO ratio for the 706-keV transition in band 2 has not been measured due to insufficient intensity in the DCO matrix, although a stretched quadrupole assignment follows from the arguments listed above. For the 415- and 559-keV γ rays, stretched $E1$ assignments are proposed, which implies opposite parity for band 2 with respect to bands 3 and 4. These assignments are further supported by the theoretical interpretation of band 3; see Sec. IV C.

The spin values for states in band 3 are consistent with the odd-*A* Te systematics. The bandhead of band 3 has a $(7/2^+)$ spin in agreement with the value proposed in Refs. [7,8] for the corresponding level in ^{109}Te. Spin assignments for the bandheads of bands 1 and 3 are supported by the observation of the 723-keV isomeric transition (see discussion in Sec. IV G). The 117-keV transition which decays out of the

TABLE I. Properties of γ rays observed in the GAMMASPHERE ^{111}Te experiment.

E_γ [a] (keV)	I_γ (%)	DCO ratio	I_i^π	→	I_f^π	Multipolarity	Band
117.1	23.0(3.0)	0.5(2)	$(7/2^+)$	→	$(5/2^+)$	$M1/E2$	3
273.2	1.8(0.4)	0.5(4)	$(21/2^-)$	→	$23/2^-$	$M1/E2$	2
342.4	1.4(0.3)		$(19/2^+)$	→	$(17/2^+)$	$M1/E2$	3
358.4	1.0(0.3)		$(27/2^-)$	→	$27/2^-$	$M1/E2$	6
364.7	2.0(0.3)	0.5(2)	(37/2)	→	$35/2^-$	$\Delta I=1$	5
373.3	1.8(0.4)		$(25/2^-)$	→	$(23/2^-)$	$M1/E2$	2
376.7	1.8(0.4)		$(21/2^-)$	→	$(19/2^-)$	$M1/E2$	2
415.0	4.9(0.7)	0.6(2)	$(21/2^-)$	→	$(19/2^+)$	$E1$	2
429.0	1.3(0.3)	0.5(2)	$(29/2^-)$	→	$(27/2^-)$	$M1/E2$	2
433.3	1.4(0.4)		$(17/2^-)$	→	$19/2^-$	$M1/E2$	2
434.6	1.8(0.3)		$(27/2^+)$	→	$(23/2^+)$	$E2$	4
451.3	2.5(0.6)		$(31/2^+)$	→	$(29/2^-)$	$E1$	4
458.8	1.6(0.3)	0.4(2)	$(33/2^-)$	→	$(31/2^-)$	$M1/E2$	2
534.7	0.7(0.3)		$(17/2^+)$	→	$(15/2^+)$	$M1/E2$	3
539.1	100.0(4.0)	1.1(1)	$15/2^-$	→	$11/2^-$	$E2$	1
555.1	1.8(0.3)		$(21/2^-)$	→	$(17/2^-)$	$E2$	2
558.8	5.6(0.7)	0.4(2)	$(27/2^+)$	→	$(25/2^-)$	$E1$	4
576.6	5.3(0.7)	1.3(3)	$(27/2^+)$	→	$(23/2^+)$	$E2$	4
605.0	5.5(0.7)	1.2(2)	$(23/2^-)$	→	$23/2^-$	$M1/E2$	6
622.1	3.7(0.5)	0.43(13)	(33/2)	→	$31/2^-$	$\Delta I=1$	5
637.8	1.5(0.3)		$(13/2^+)$	→	$(11/2^+)$	$M1/E2$	3
650.9	6.9(0.8)		$(9/2^+)$	→	$(7/2^+)$	$M1/E2$	3
662.3	16.4(1.1)	0.50(8)	(29/2)	→	$27/2^-$	$\Delta I=1$	5
682.9	95.0(4.0)	1.1(1)	$19/2^-$	→	$15/2^-$	$E2$	1
692.7	10.9(0.6)	1.0(3)	$(31/2^+)$	→	$(27/2^+)$	$E2$	4
706.0	10.3(0.6)		$(25/2^-)$	→	$(21/2^-)$	$E2$	2
715.0	79.0(3.0)	}1.0(1)	$23/2^-$	→	$19/2^-$	$E2$	1
717.8	15.4(1.6)		(37/2)	→	(33/2)	$E2$	5
744.6	5.3(0.7)	1.0(3)	$(27/2^-)$	→	$(23/2^-)$	$E2$	6
751.6	6.0(0.7)		$(13/2^+)$	→	$(9/2^+)$	$E2$	3
760.1	3.8(0.5)		$(31/2^-)$	→	$(27/2^-)$	$E2$	6
761.8	3.1(0.5)			→	(41/2)		5
765.0	21.0(3.0)	0.9(2)	$(11/2^+)$	→	$(7/2^+)$	$E2$	3
773.0	3.7(0.4)		$(17/2^+)$	→	$(13/2^+)$	$E2$	3
778.7	1.8(0.2)						
788.5	11.1(0.7)	1.0(3)	$(35/2^+)$	→	$(31/2^+)$	$E2$	4
788.9	2.0(0.7)		$(33/2^-)$	→	$(29/2^-)$	$E2$	2
800.1	7.0(0.9)		$(29/2^-)$	→	$(25/2^-)$	$E2$	2
838.1	1.8(0.5)			→	$(39/2^+)$		
857.1	7.7(0.9)	1.1(3)	$(39/2^+)$	→	$(35/2^+)$	$E2$	4
870.6	1.1(0.3)						
875.1	17.3(1.2)	}1.1(2)	$(15/2^+)$	→	$(11/2^+)$	$E2$	3
878.2	12.8(1.3)		(19/2+)	→	(15/2+)	$E2$	3
883.7	1.8(0.3)						
900.4	1.3(0.3)						5
919.0	6.0(0.8)	}0.9(1)	(41/2)	→	(37/2)	$E2$	5
922.4	13.5(1.5)		(33/2)	→	(29/2)	$E2$	5
938.9	2.1(0.4)						
963.1	15.5(1.6)	1.0(1)	$31/2^-$	→	$27/2^-$	$E2$	1
975.1	5.8(0.8)	1.0(2)	$35/2^-$	→	$31/2^-$	$E2$	1
989.0	3.5(0.7)		$(21/2^-)$	→	$19/2^-$	$M1/E2$	2
991.1	51.0(2.0)	1.1(1)	$27/2^-$	→	$23/2^-$	$E2$	1
1023.6	3.8(0.5)		$(43/2^+)$	→	$(39/2^+)$	$E2$	4
1046.2	1.1(0.3)						
1050.5	2.1(0.5)		$(47/2^+)$	→	$(43/2^+)$	$E2$	4
1103.3	5.8(0.8)	1.0(3)	$(23/2^+)$	→	$(19/2^+)$	$E2$	4
1112.7	1.4(0.4)		$(39/2^-)$	→	$35/2^-$	$E2$	1
1117.8	1.8(0.4)		$(17/2^-)$	→	$15/2^-$	$M1/E2$	2
1119.1	3.5(0.7)	1.1(3)	$(31/2^-)$	→	$27/2^-$	$E2$	6
1135.7	1.1(0.3)		$(51/2^+)$	→	$(47/2^+)$	$E2$	4
1245.4	1.8(0.4)		$(23/2^+)$	→	$(19/2^+)$	$E2$	4
1295.1	2.1(0.4)		$(19/2^-)$	→	$15/2^-$	$E2$	6
1305.4	1.4(0.3)						5
1320.7	2.3(0.5)		$(23/2^-)$	→	$19/2^-$	$E2$	6

[a]Energies are typically accurate to within ± 0.3 keV.

TABLE II. Properties of selected γ rays observed in the Stony Brook ^{111}Te experiment.

E_γ [a] (keV)	I_γ (%)	$A=W(30°)/W(90°)$	I_i^π	→	I_f^π	Multipolarity	Band
285.5	7(4)		$(9/2^+)$	→	$(7/2^+)$	$M1/E2$	3
421.1	1(1)		$(7/2^+)$	→	$(7/2^+)$	$M1/E2$	3
538.4	3(2)		$(7/2^+)$	→	$(5/2^+)$	$M1/E2$	3
723.3	100(9)	1.35(15)	$11/2^-$	→	$(7/2^+)$	$M2/E3$	1
823.6	29(7)		$(9/2^+)$	→	$(5/2^+)$	$E2$	3

[a]Energies are typically accurate to within ± 0.3 keV.

bandhead of band 3 has a DCO ratio consistent with $\Delta I \leqslant 1$ which suggests a $(5/2^+)$ spin for the state with the lowest energy observed in this experiment. A ground state spin of $(5/2^+)$ in ^{111}Te was suggested in Ref. [10] and adopted in Ref. [11]. The value is also consistent with the $(5/2^+)$ ground state spin of ^{109}Te proposed in Refs. [7,8]. It should be noted, however, that $(7/2^+)$ was proposed as the ground state spin in ^{113}Te [12].

C. Decay of the $11/2^-$ state

The energy of the $11/2^-$ bandhead of band 1 is 723 keV above the energy of the $(7/2^+)$ bandhead of band 3. The $11/2^-$ to $7/2^+$ decay requires a γ ray with multipolarity $M2/E3$; the Weisskopf estimate for such a transition in ^{111}Te is $\tau \approx 10$ ns for an $M2$ and $\tau \approx 22$ μs for an $E3$, respectively. The GAMMASPHERE data suggested that the $11/2^-$ state is an isomer with a mean lifetime in the tens of nanoseconds range. In gates set on transitions of band 1, the $(7/2^+) \rightarrow (5/2^+)$ 117-keV γ ray was observed. The 723-keV transition connecting the $11/2^-$ and $7/2^+$ levels was observed but its intensity could not be estimated due to strong contamination from the doublet at 715 and 718 keV (the energy resolution at that energy was ~ 5 keV due to Doppler broadening). The decay of the $11/2^-$ state to the $7/2^+$ state by an $M2$ transition was observed in ^{115}Te, where $\tau = 10.8(3)\mu$s was measured [13]. Assuming the same $B(M2)$ in ^{111}Te as in ^{115}Te, a $\tau \sim 110$ ns for the lifetime of the $11/2^-$ isomeric state in ^{111}Te can be estimated.

The lifetime experiment performed at Stony Brook resulted in prompt-prompt, prompt-delayed, and delayed-delayed coincidence measurements within the 106-ns beam sweeping period (which is the fundamental beam sweeping period for the Stony Brook LINAC accelerator). The prompt spectrum gated on the delayed 723-keV γ ray is shown in the upper panel of Fig. 3 while the delayed spectrum gated on the prompt 539-keV γ ray is shown in the lower panel of the same figure. The time spectrum measured for the 723-keV γ ray with the 106-ns beam sweeping period is shown in the upper panel of Fig. 4 with the prompt and the delayed re-

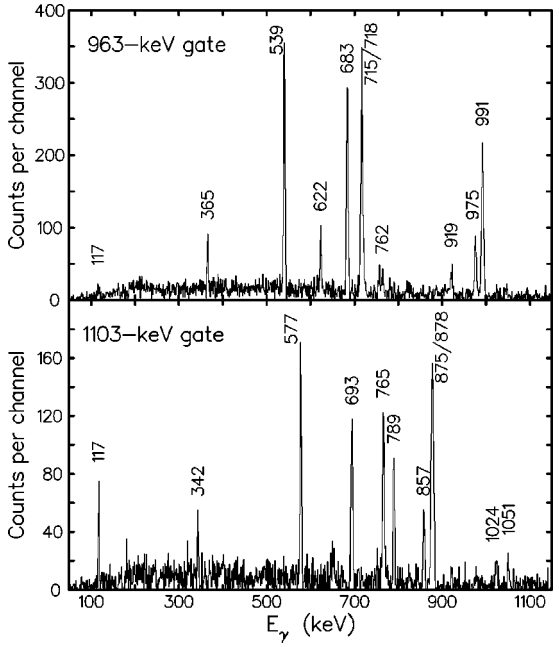

FIG. 2. Coincidence spectra gated on the 963-keV (top) and 1103-keV (bottom) γ-ray transitions, taken from the $4pn$-gated GAMMASPHERE/MICROBALL matrix.

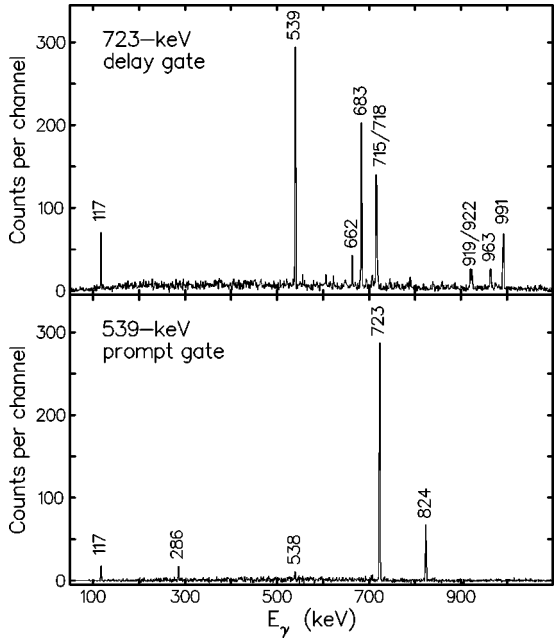

FIG. 3. Prompt γ-ray spectrum gated on the 723-keV delayed γ-ray transition (top) and delayed γ-ray spectrum gated on the 539-keV prompt γ-ray transition (bottom). Spectra were acquired using the Stony Brook six-Ge-detector array. A fraction of the 117-keV transition is seen in the delayed 723-keV gate due to a broadening of the prompt time resolution function at low γ-ray energy.

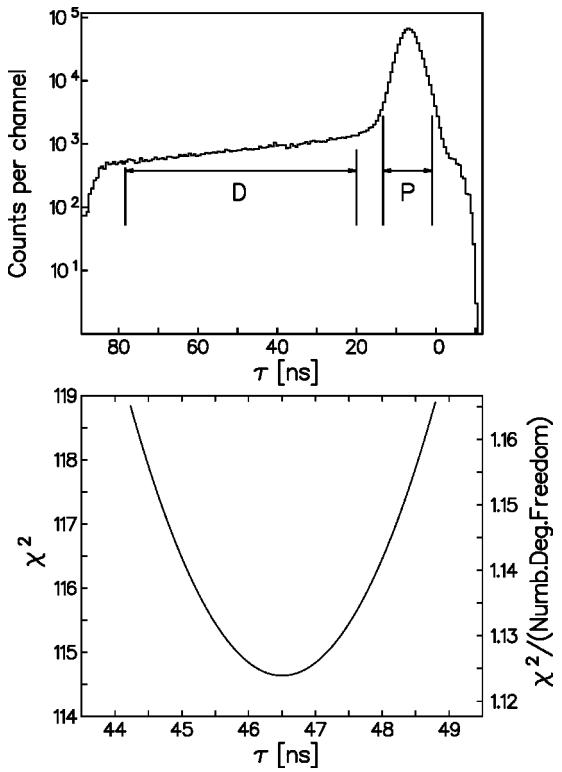

FIG. 4. Top: decay curve measured for the 723-keV γ ray with a 106-ns beam sweeping period. Prompt (P) and delayed (D) regions in the time spectrum are marked. Bottom: results of the least squares fit to the decay curve measured with a 318-ns beam sweeping period.

gions marked on the plot. Based on these spectra, the $11/2^-$ state is presumed to decay through an unobserved 16-keV $E1\,\gamma$ ray to the $(9/2^+)$ state at 0.824 MeV, in addition to the 723-keV $M2$ transition to the $(7/2^+)$ state in band 3 (see Fig. 1). The existence of the nonyrast $(7/2^+)$ and $(9/2^+)$ states fed by the decay of the $11/2^-$ isomer was confirmed by the coincidence relationships between 286-, 421-, and 538-keV γ rays observed in the GAMMASPHERE data.

The lower panel of Fig. 4 shows the result of a least squares fit applied to the data measured with the 318-ns beam sweeping period. The beam sweeping period of 318 ns was achieved by deflecting two out of every three beam pulses away from the target. The effects due to the imperfect beam deflecting (dark current) were taken into account during the fitting procedure. The amount of dark current was on the order of 5% of the total beam current. The normalized χ^2 at the minimum of the fit is χ^2/(number of degrees of freedom)$=1.122$. Based on this measurement, a value of $\tau=46.5(2.0)$ ns is deduced as the mean lifetime of the $11/2^-$ isomer.

In the timing data recorded with the 106-ns beam sweeping period, the decay of the 6^+ isomeric state in ^{108}Sn produced in the $\alpha 4p$ channel was observed. A mean lifetime of $\tau=7.0(2)$ ns was extracted for this state, which agrees with the $\tau=7.3(4)$ ns value adopted in Nuclear Data Sheets (based on Ref. [14]) and confirms the time calibration. The time calibration for the run with 318-ns beam sweeping period was checked by measuring the time interval between beam pulses without the deflector.

The partial lifetimes for the $M2$ and the $E1$ decays of the $11/2^-$ isomer in ^{111}Te can be obtained knowing the branching ratio of the 16- and 723-keV transitions. This branching was measured using the sum of the delayed spectra gated on prompt 539- and 683-keV transitions. The intensity of the 16-keV transition (including electron conversion) was estimated as equal to the sum of intensities of the 286- and 824-keV γ-ray transitions. The measured value $\lambda(16\text{ keV})/\lambda(723\text{ keV})=0.36(9)$ gives transition probabilities $1/\lambda(M2)=63(5)$ ns for the 723-keV transition and $1/[\lambda(E1)+\lambda(\text{electron conversion})]=176(14)$ ns for the 16-keV decays.

The asymmetry of the angular distribution A, defined as the ratio of the intensity observed by the detectors at $\sim 30°$ to the intensity observed by the detectors at $\sim 90°$, was measured as a function of time for the 723-keV transition. It was observed that the asymmetry varies only slightly with time, which indicates that the spin alignment is well preserved during the measurement. The spin deorientation effects are, therefore, not expected to significantly influence the measured value of the $11/2^-$ isomer lifetime. If the asymmetry is extrapolated to the time coinciding with the beam burst, a value of $A=1.35(15)$ is obtained. This value is consistent with the $M2$ assignment proposed for the 723-keV transition and can be reproduced in calculations with a reasonable value of the spin alignment parameter $\sigma/I=0.4$. Present data are too limited to make any conclusion about a possible $E3$ admixture, although the Weisskopf estimate discussed above suggests that it is negligible.

IV. DISCUSSION

A. Core-quasiparticle calculations

Theoretical investigations of odd-A Te isotopes have shown that the low-lying negative-parity levels can be understood in terms of core-particle coupling [15,16]. In the present study, the core-quasiparticle coupling (CQPC) model was used to calculate both negative- and positive-parity levels expected at low excitation energy. The same model has been successfully applied recently in the mass-130 region [17,18]. The Hamiltonian of the model is the sum of contributions from the core, from the odd particle (odd hole), and from interactions. The interaction part includes pairing and quadrupole-quadrupole (Q-q) interactions between the core and the valence particle (hole). The Q-q Hamiltonian is calculated using the reduced matrix elements of the $E2$ operator for single-particle orbitals and the reduced matrix elements of the $E2$ operator between the core states. The matrix elements of the core are input parameters of the model, allowing investigations of the single-particle coupling with various cores.

In the present study, two sets of matrix elements for the core were considered: the first set calculated according to the axially symmetric rigid-rotor model [19] and the second calculated according to the harmonic-vibrator model [20]. For both models, a $B(E2,0_1^+\rightarrow 2_1^+)=0.50\ e^2\,\mathrm{b}^2$ was assumed

TABLE III. Selected core parameters used in the CQPC calculations. The reduced matrix elements of the $E2$ operator were calculated assuming a deformation $\beta_2=0.186$ for the rigid rotor or a square root of the mean square deformation $\sqrt{\beta_2^2}=0.186$ for the harmonic vibrator. For the rigid rotor, reduced matrix elements are calculated up to the terms proportional to β_2 ($Q_0=2.247$ e b). For the harmonic vibrator, the transitional matrix elements are calculated up to the terms proportional to $\sqrt{\beta_2^2}$ while the diagonal matrix elements are calculated up to the terms proportional to β_2^2.

				Rigid rotor			Harmonic vibrator		
I_i^π	I_f^π	$E(I_i^\pi)$ (MeV)	$E(I_i^\pi)$-$E(I_f^\pi)$ (MeV)	$\langle I_i^\pi\|\|E2\|\|I_f^\pi\rangle$ (e b)	$B(E2,I_i^\pi\rightarrow I_f^\pi)$ (e^2 b^2)	$Q(I_i^\pi)$ (e b)	$\langle I_i^\pi\|\|E2\|\|I_f^\pi\rangle$ (e b)	$B(E2,I_i^\pi\rightarrow I_f^\pi)$ (e^2 b^2)	$Q(I_i^\pi)$ (e b)
0^+	0^+	0.000		0.000		0.000	0.000		0.000
2^+	0^+		0.657	0.709	0.100		0.709	0.100	
2^+	2^+	0.657		-0.847		-0.642	-0.080		-0.060
4^+	2^+		0.744	1.136	0.144		1.345	0.200	
4^+	4^+	1.401		-1.084		-0.817	-0.160		-0.120
6^+	4^+		0.824	1.433	0.158		1.979	0.300	
6^+	6^+	2.225		-1.289		-0.899	-0.259		-0.180
8^+	6^+		1.062	1.677	0.165		2.613	0.400	
8^+	8^+	3.287		-1.469		-0.946	-0.374		-0.240

following the predictions given in Ref. [21]. This value corresponds to a deformation $\beta_2=0.186$ for a rigid rotor or a square root of the mean square deformation $\sqrt{\beta_2^2}=0.186$ for a harmonic vibrator. The core subspace was limited to the yrast states with $I^\pi=0^+$, 2^+, 4^+, 6^+, and 8^+. For both core types, the energies of the yrast states were fixed to the experimental energies observed in ^{110}Te [22]. Such a truncation of the core basis limits the accuracy of the calculated spectrum in an odd-A nucleus. Therefore only a few selected low energy levels in ^{111}Te were compared to the results of the CQPC calculations. The information about core states is summarized in Table III.

The single-particle energy spectrum for neutrons, shown in Fig. 5, was calculated using a spherically symmetric Woods-Saxon potential with the universal parametrization [23]. Matrix elements between the single-particle orbitals were calculated using harmonic-oscillator wave functions.

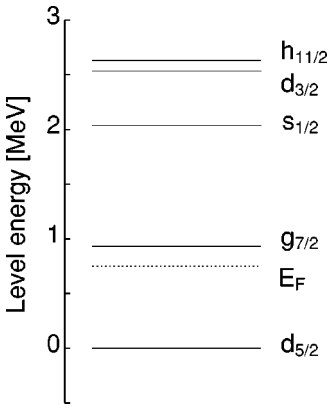

FIG. 5. Single-particle energy level spectrum for neutrons calculated for ^{111}Te using a spherically symmetric Woods-Saxon potential with the universal parametrization [23]. The position of the Fermi level is marked.

The position of the Fermi level was adjusted to reproduce the number of neutrons in ^{111}Te. The energy of the $\nu h_{11/2}$ orbital in ^{111}Te with respect to the Fermi level ($\sim$2 MeV) is large compared to the estimated pairing gap $\Delta_\nu=135/A\approx 1.2$ MeV. In such cases, core-quasiparticle coupling gives results very close to the core-particle coupling model, which neglects the pairing interactions. It is therefore expected that the results for the negative-parity levels are not very sensitive to the exact energy of the $h_{11/2}$ neutron with respect to the Fermi level. This is not the case for the positive-parity levels, where small shifts in single-particle energies (especially for the $d_{5/2}$ and $g_{7/2}$ orbitals) significantly alter the calculated spectrum. One should also note that the structure of low-energy collective states in even-A Te cores involves mostly particle-hole excitations between positive-parity orbitals; therefore, the separation of the core and the valence particle is expected to work better for negative-parity states than for positive-parity states.

In the CQPC calculations, the value of the Q-q coupling constant was varied to obtain a good fit for negative-parity levels (see Sec. IV B). The deduced value $\chi_{Q\text{-}q}\approx -10$ MeV/b^2 may be compared to the estimate made in Ref. [24],

$$\chi_{Q\text{-}q}=-240A^{-5/3}b_o^{-4}\ \text{MeV},$$

where $b_o=\sqrt{\hbar/m_n\omega}$ is the oscillator parameter. This gives $\chi_{Q\text{-}q}=-40$ MeV/b^2 for ^{111}Te. In Ref. [25], however, it is suggested that the above parametrization overestimates $\chi_{Q\text{-}q}$, and the parametrization

$$\chi_{Q\text{-}q}=-0.0251b_o^{-4}\ \text{MeV}$$

is proposed, which gives $\chi_{Q\text{-}q}=-10$ MeV/b^2 for ^{111}Te in excellent agreement with the value deduced from the calculations.

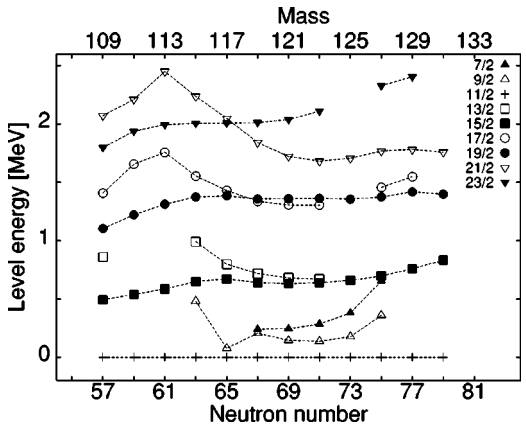

FIG. 6. Systematics of the energies measured for the low-lying negative-parity states in odd-*A* Te isotopes, plotted relative to the bandheads. Energy levels were adopted from Ref. [7] and Ref. [26] for ^{109}Te and ^{113}Te, respectively, and from the Nuclear Data Sheets for ^{115}Te—^{131}Te.

B. Bands 1 and 2

Bands built on the $\nu h_{11/2}$ orbital are observed systematically in the odd-*A* Te isotopes. The energies of the low-lying negative-parity band members (relative to the bandheads) for the $^{109-131}$Te isotopes are presented in Fig. 6. In the current study, bands 1 and 2 in ^{111}Te at low spin are interpreted as the favored and unfavored signatures, respectively, of the $h_{11/2}$ band. The interpretation is consistent with the trends presented in Fig. 6.

The results of CQPC calculations for low-lying negative-parity states in ^{111}Te, using the rigid-rotor core and different values of the Q-q coupling constant $\chi_{Q\text{-}q}$, are shown in the top panel of Fig. 7. Good agreement between experimental and theoretical energies of the $15/2^-$, $17/2^-$, and the $19/2^-$ states is obtained for $\chi_{Q\text{-}q} \approx -10$ MeV/b^2. The CQPC calculations predict large excitation energies for the states which are not fully aligned ($9/2^-$ and $13/2^-$); this may explain why these nonyrast states were not observed experimentally.

The calculations with a vibrational core did not resemble the experimental results for any considered value of $\chi_{Q\text{-}q}$; the calculated energies of the $15/2^-$, $17/2^-$, and $19/2^-$ states vary only slightly as $\chi_{Q\text{-}q}$ increases. This behavior is very different from the trend calculated for coupling with a rigid rotor. One of the reasons why this difference occurs is the fact that the diagonal matrix elements of the $E2$ operator, which contribute significantly to the Hamiltonian of the Q-q interactions, are an order of magnitude smaller for vibrational states than for rotational states (see Table III). Additional calculations with an extended basis for the harmonic-vibrator model were performed to investigate the influence of the truncated core basis on the calculated level energies for an odd-*A* nucleus. The extended basis consisted of the zero-, one-, two-, and three-phonon multiplets and the four-phonon 8^+ state. A degeneracy of the phonon multiplets was assumed in these calculations to obtain the energies of unknown nonyrast states. The results which are shown in the lower panel of Fig. 7 correspond to the calculation with the extended basis and do not differ significantly from those obtained with the basis which included yrast states only.

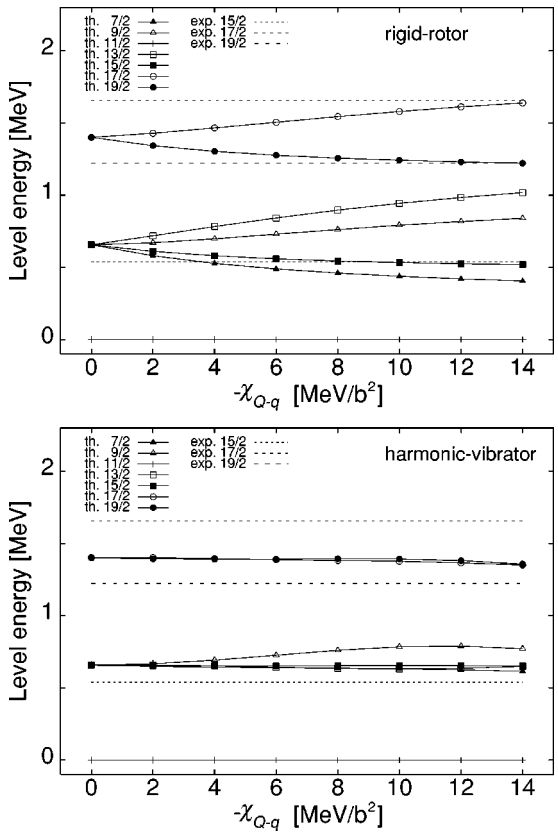

FIG. 7. Energies relative to the bandhead for low-lying negative-parity states in ^{111}Te as a function of the Q-q interaction strength, $\chi_{Q\text{-}q}$, calculated with rigid-rotor core (top) and harmonic-vibrator core with an extended basis containing nonyrast states (bottom). The experimental energies for $15/2^-$, $17/2^-$, and $19/2^-$ are marked by horizontal dashed lines. Good agreement between experimental and theoretical energies for these states is observed as displayed in the top panel for $\chi_{Q\text{-}q} \approx -10$ MeV/b^2.

The good agreement between the experiment and the calculations with a rigid-rotor core, and lack of agreement between the experiment and the calculations with a harmonic-vibrator core, suggests sizable negative spectroscopic quadrupole moments for the core yrast states (see Table III). The values of the spectroscopic quadrupole moments measured [1] or calculated for yrast states of heavier even-*A* Te nuclei [see Ref. [27] for Hartree-Fock-Bogliubov (HFB) or Ref. [28] for interacting boson model (IBM) approach] are consistent with this conclusion. The effect may also be explained by the deformation-driving force exerted on the soft core by the odd $h_{11/2}$ neutron.

Because of the good agreement achieved for band 1 using the rotational core-particle coupling model, additional comparisons with cranked shell model calculations were made. The upper panel of Fig. 8 shows spin values measured in the experiment as a function of rotational frequency, along with the values calculated using the total Routhian surface (TRS) model [29]. The theory reproduces the experimental curve reasonably well, attributing the alignment at $\hbar\omega \approx 0.5$ MeV to neutrons. Further investigation of the quasineutron

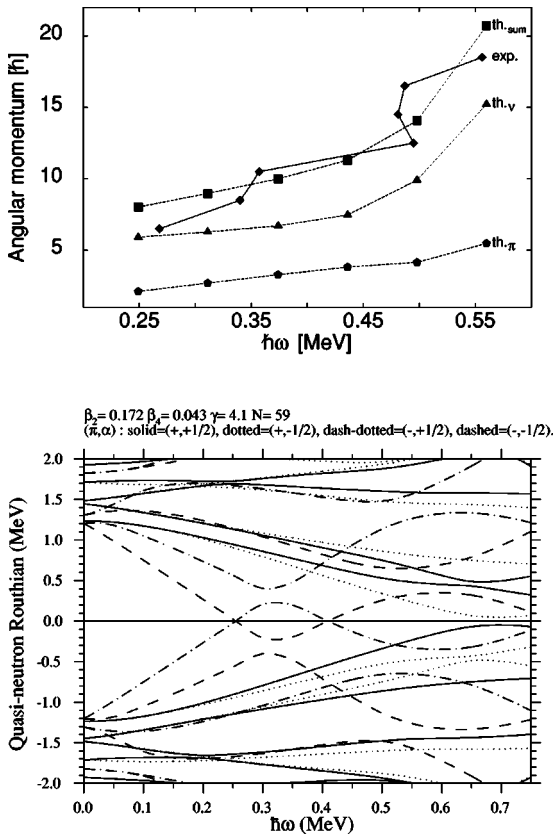

FIG. 8. Top: spin as a function of rotational frequency for band 1 (diamonds) and as calculated using the TRS model for the lowest-energy band with negative parity and negative signature (squares). The neutron contribution to the total calculated spin is marked with triangles and the proton contribution is marked with pentagons. Bottom: quasineutron Routhians calculated for the $\nu h_{11/2}$ band in ^{111}Te at the deformation parameters corresponding to the minimum of the total Routhian at $\hbar\omega = 0.498$ MeV.

Routhians shown in the lower panel of Fig. 8 suggests that at $\hbar\omega \approx 0.5$ MeV, the gain in aligned angular momentum is generated by a $\nu h_{11/2}$ alignment. The angular momentum for high-spin states appears, in such a case, to be generated in a different way in ^{111}Te than in the ^{109}Sn isotone [30], where high-spin negative-parity states were interpreted as resulting from a $\nu h_{11/2}$ orbital coupled to a $\nu(g_{7/2}d_{5/2})$ pair. This may be explained by the higher deformation expected for ^{111}Te with respect to ^{109}Sn and the decrease of the high-j orbital energy with increasing deformation.

C. Band 3

The systematic properties of low-lying positive-parity levels in odd-A Te are shown in Fig. 9. These levels form a band built on a $7/2^+$ state which becomes the ground state for ^{115}Te. It is expected that the structure of the band involves mixed $d_{5/2}$ and $g_{7/2}$ orbitals. The systematics do not include the heavier Te isotopes where the influence of $s_{1/2}$ and $d_{3/2}$ neutron orbitals becomes important.

The results of CQPC calculations with $\chi_{Q\text{-}q} = -10$ MeV/b^2 and the single-particle spectrum shown in Fig. 5 for two different core types are presented in Fig. 10.

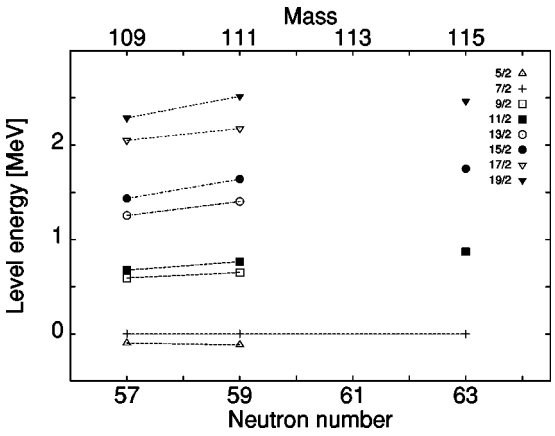

FIG. 9. The systematics of the energies measured for the low-lying positive-parity states relative to the $7/2^+$ bandhead in odd-A Te isotopes. Data are taken from Refs. [7,8] for ^{109}Te and from Nuclear Data Sheets for ^{115}Te.

The spectra calculated with rigid-rotor core and with harmonic-vibrator core differ only in minor details. Both sets of calculations predict the existence of two $\Delta I = 1$ bands with specific signature splittings built on mixed $d_{5/2}$ and $g_{7/2}$ orbitals. The band built predominantly on $d_{5/2}$ is nonyrast with respect to the band built predominantly on $g_{7/2}$. This conclusion agrees well with the data (see Fig. 1), especially with the results of the Stony Brook experiment where low-energy nonyrast positive-parity states were observed to be populated from the decay of the $11/2^-$ isomer. Nonyrast positive-parity states at low energies were also observed in ^{109}Te [7,8]. Both sets of calculations fail to predict the $5/2^+$ as a ground state, although the $5/2^+$ bandhead may be shifted below the $7/2^+$ state by a ~ 0.4 MeV shift of the Fermi level towards the $d_{5/2}$ state. Theoretical results are in qualitative agreement with the experimental data, suggesting the $g_{7/2}$ orbital as the single-particle configuration for band 3. The interacting boson-fermion model (IBFM) calculation performed in Ref. [8] for ^{109}Te gave results consistent with those presented above.

D. Band 4

The bandhead of band 4 lies more than 4 MeV above the bandhead of band 3 [$E(27/2^+) = 4.197$ MeV] and is hence expected to be a three-quasiparticle state. The proposed positive parity for this band suggests a structure involving two negative-parity $h_{11/2}$ and one positive-parity $(g_{7/2}d_{5/2})$ quasineutron. The corresponding negative-parity band built on an $h_{11/2}$ quasineutron coupled to a $(g_{7/2}d_{5/2})$ quasineutron has been observed in both ^{110}Te [22] and ^{112}Te [31]. These bands were shown to have a 9^- bandhead at excitation energies of 3.739 MeV and 3.629 MeV, respectively.

Standard TRS calculations performed for positive parity and negative signature predicts a structure with aligned neutrons existing at rotational frequencies above ~ 0.35 MeV. The calculations for band 4 (see Fig. 11) do not reproduce the spin vs rotational frequency curve as well as for band 1. The deformation $\beta_2 \sim 0.16$ predicted by the TRS calculations

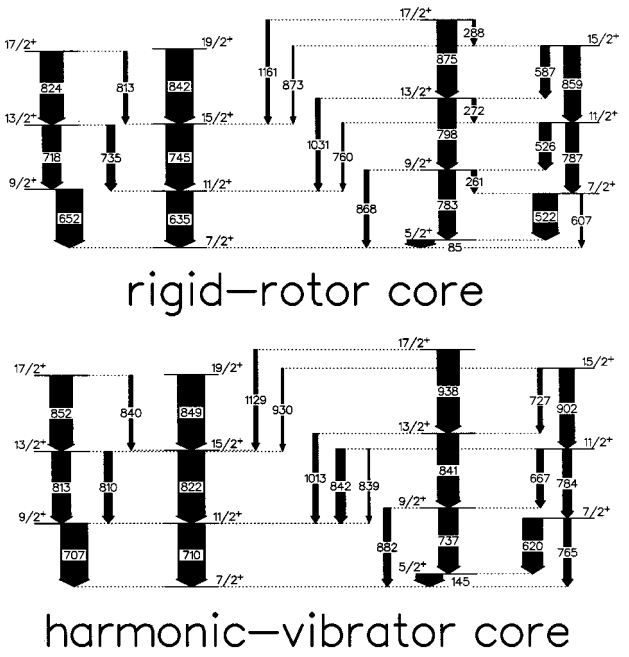

FIG. 10. The results of CQPC calculations with rigid-rotor core (top) and harmonic-vibrator core (bottom) for selected positive-parity levels at low excitation energy in ^{111}Te. The widths of the arrows represent calculated relative intensities of the γ transitions.

may be too small to account for the observed spin vs frequency dependence.

E. Band 5

The band in ^{109}Te which is an analog of band 5 in the current ^{111}Te study was discussed recently in Refs. [7,9] as a possible example of a rotationally stabilized collective octupole excitation coupled to the odd $h_{11/2}$ neutron. Enhancements of the octupole strength are expected in the mass $A \sim 110$ region due to the proximity of the $h_{11/2}$ and $d_{5/2}$ orbitals to the Fermi level [32]. The interpretation in ^{109}Te is based on the assumption that the links to the yrast band are enhanced $E1$ transitions. It was pointed out in Refs. [7,33] that polarization measurements are needed in neutron-deficient Te isotopes to firmly support the hypothesis of octupole collectivity.

F. Band 6

The $(23/2^-)$ state of the bandlike structure labeled band 6 is likely to result from the coupling of the $\nu h_{11/2}$ orbital to the 6^+ state of the even-A core. Figure 12 shows the low-energy states known in ^{110}Te and ^{112}Te compared to bands 1 and 6 in ^{111}Te. There are three and two nearly degenerate 6^+ states (within a 300-keV range) in ^{110}Te and ^{112}Te, respectively. Such near degeneracy is not explained by simple collective models. According to the harmonic-vibrator model, for example, the second 6^+ state should have the same energy as the first 8^+ state. On the other hand, the two quasiparticle 6^+ isomers resulting from the $\nu(g_{7/2}d_{5/2})^2$ coupling are well known in neutron-deficient even-A Sn isotopes. The energies of these states coincide with the observed nonyrast 6^+ states in the related even-A Te isotones, $E(6_1^+)=2364$ keV in ^{108}Sn and $E(6_1^+)=2480$ keV in ^{110}Sn, while $E(6_2^+)=2440$ keV in ^{110}Te and $E(6_2^+)=2449$ keV in ^{112}Te. In heavier Te isotopes, the nonyrast 6^+ states were explained as resulting from a $\pi(g_{7/2}d_{5/2})^2$ coupling (see Ref. [34]). The hypothesis of a single-particle character for these nonyrast 6^+ states seems, therefore, well justified.

Single-particle configuration assignments for the 6^+ states of interest in ^{110}Te and ^{112}Te have not been clearly identified. Arguments based on systematics should be taken with caution when extrapolating from isotopes with larger neutron numbers. Indeed the $\nu(g_{7/2}d_{5/2})^2$ configuration is unlikely in heavier Te isotopes due to the high position of the Fermi level, but for $A \sim 110$ the Fermi energy for protons and neutrons becomes comparable. The fact that two nonyrast 6^+ states are observed in ^{110}Te may indicate that both $\nu(g_{7/2}d_{5/2})^2$ and $\pi(g_{7/2}d_{5/2})^2$ configurations are observed. Further experimental effort, especially information on magnetic moments of these states, is needed for a firm assignment.

Excitation energies and spins for levels forming band 6 in ^{111}Te fit well to the systematics shown in Fig. 12. For band 6, a three-quasiparticle configuration is proposed involving the $\nu h_{11/2}$ orbital coupled to the nonyrast states of the core shown in Fig. 12.

G. Systematics of the $11/2^- \rightarrow 7/2^+$ decay

The energy systematics of the $11/2^-$ state with respect to the $7/2^+$ state in the odd-A Te neighbors of ^{111}Te is presented in the upper panel of Fig. 13. The $B(M2, 11/2^- \rightarrow 7/2^+)$ strengths in odd-A Te and Sn isotopes are presented in the lower panel of Fig. 13. The $11/2^- \rightarrow 7/2^+ M2$ decay has not yet been reported in ^{113}Te. An estimate for ^{113}Te resulting from the systematics presented in Fig. 13 is $E \approx 490$ keV for the energy of the $11/2^-$ state relative to the $7/2^+$ state and $1/\lambda \approx 0.5$ μs for the $M2$ transition lifetime.

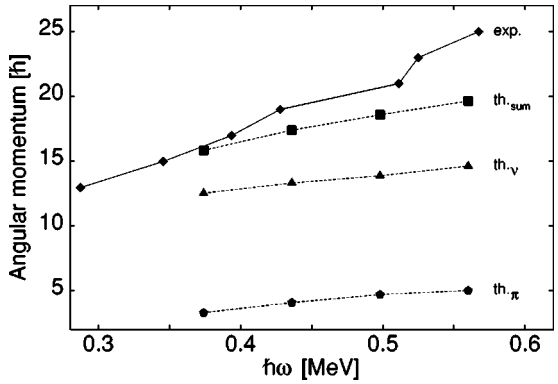

FIG. 11. Spin as a function of rotational frequency for band 4 (diamonds) and as calculated using the TRS model for the lowest-energy three-quasiparticle band with positive parity and negative signature (squares). The neutron contribution to the total calculated spin is marked with triangles, and the proton contribution is marked with pentagons.

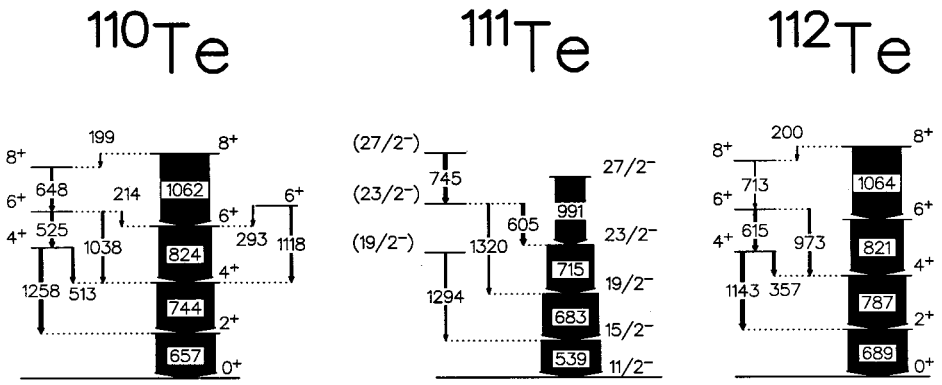

FIG. 12. Low-spin yrast and nonyrast states in ^{110}Te and ^{112}Te compared to negative-parity states of bands 1 and 6 in ^{111}Te. The widths of the arrows in each level scheme represent relative intensities of the γ-ray transitions.

The Weisskopf estimate for a $B(M2)$ reduced probability in the $A\sim110$ region is $\sim38\mu_N^2\,\mathrm{fm}^2$. The systematics presented in Fig. 13 shows that $M2$ transitions in odd-A Te and Sn are hindered by a factor between 5 and 10. A clear correlation between $M2$ strength and neutron number exists with the $M2$ strength being most hindered near the neutron midshell. The hindrance factor in the Sn isotopes was discussed in Ref. [35] as arising from pairing effects, with the trend explained by a change in pairing occupation factors due to the position of the neutron Fermi level. In Ref. [36] the absolute value of those hindrances was discussed as resulting from the quenching of gyromagnetic factors.

The $M2$ hindrances in Te are $\sim40\%$ larger than those in corresponding Sn isotones with a similar trend as a function of neutron number. This difference is likely to be caused by the increased deformation of Te isotopes compared to Sn isotopes because the quadrupole-quadrupole interaction perturbs the energy levels more strongly in deformed nuclei. A possible scenario, which is supported by CQPC calculations, relies on the observation that as the deformation increases the wave functions of the observed $11/2^-$ and $7/2^+$ levels pick up components involving the 2^+ and 4^+ core states. An increasing amplitude of those admixtures would result in a smaller value for the calculated $M2$ matrix element. According to this scenario, the effect is expected to be stronger for weakly deformed Te than for near spherical Sn nuclei. Further experimental and theoretical studies, including measurement of the $M2$ strength ^{113}Te, are needed to address the underlying physics in detail.

V. SUMMARY

Experimental information regarding excited states in ^{111}Te was extended in the current study from the previous work in Ref. [6]. Charged-particle and neutron tagging used in the present experiment confirmed the prior results obtained using γ-γ, γ-neutron, and γ-recoil coincidence information. The observed energy spectrum of the low-spin states was compared to the results of CQPC calculations performed with both an axially symmetric rigid-rotor core and a harmonic-vibrator core. The good agreement obtained for the negative-parity yrast states using the rigid-core calculations suggests that the core in ^{111}Te may have sizable diagonal matrix elements of the $E2$ operator. This implies the influence of the deformation-driving force of the $\nu h_{11/2}$ orbital, a sizable spectroscopic quadrupole moment of the ^{110}Te core at low spins, or both. The sizable $E2$ diagonal matrix elements in the vibrational approach would indicate a large anharmonicity. The observed properties of the yrast band are well reproduced by the TRS model based on assumed cranking. The positive-parity band observed at low spin was identified as built on a mixed $\nu(g_{7/2}d_{5/2})$ orbital. At excitation energies above ~4 MeV, a collective band assigned to the three quasineutron $(g_{7/2}d_{5/2})\otimes(h_{11/2})^2$ configuration was observed.

An $M2$ $11/2^-\rightarrow7/2^+$ isomeric transition in ^{111}Te was identified and its mean lifetime has been measured to be $\tau=46.5(2.0)$ ns. The systematics of $M2$ strength in Te and Sn isotopes have been discussed, indicating that the lowest

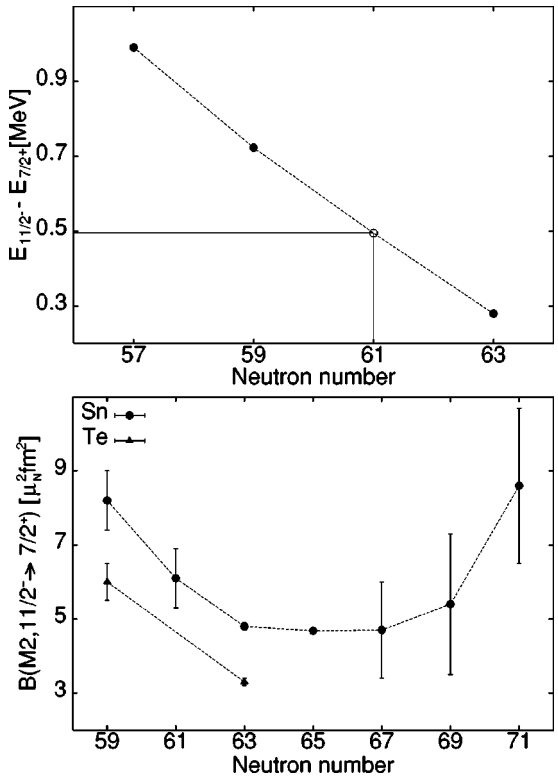

FIG. 13. Top: energy systematics of the $11/2^-$ state relative to the $7/2^+$ state in ^{109}Te, ^{111}Te, and ^{115}Te. Data were taken from Refs. [7,8] for ^{109}Te and from Ref. [13] for ^{115}Te. Bottom: systematics of the $B(M2,11/2^-\rightarrow7/2^+)$ in odd-A Te and Sn isotopes. Data were taken from Ref. [13] for ^{115}Te and from Refs. [35,36] for the Sn isotopes.

$M2$ strength is at the neutron midshell and a decrease in $M2$ strength occurs with increasing proton number. Deformation-induced mixing is likely to be responsible for the higher hindrance factor in the Te isotopes compared to the Sn isotopes with the same number of neutrons.

The $Z \sim 50$, $A \sim 110$ nuclei provide important information on the development of collectivity in the vicinity of the doubly closed shell, and it is believed that further experimental and theoretical investigations in this region would achieve progress towards a more complete understanding of the related nuclear structure.

ACKNOWLEDGMENTS

The authors would like to thank Professor Ch. Droste and Dr. J. Srebrny for the discussion concerning the CQPC calculations and Dr. C. J. Lister, Dr. S. J. Freeman, and the University of Manchester group for setting up the neutron detectors.

[1] P. Raghavan, At. Data Nucl. Data Tables **42**, 189 (1989).
[2] D. G. Sarantites, P.-F. Hua, M. Devlin, L. G. Sobotka, J. Elson, J. T. Hood, D. R. LaFosse, J. E. Sarantites, and M. R. Maier, Nucl. Instrum. Methods Phys. Res. A **381**, 418 (1996).
[3] D. C. Radford, Nucl. Instrum. Methods Phys. Res. A **361**, 297 (1995).
[4] A. Krämer-Flecken, T. Morek, R. M. Lieder, W. Gast, G. Hebbinghaus, H. M. Jeger, and W. Urban, Nucl. Instrum. Methods Phys. Res. A **275**, 333 (1989); K. S. Krane, R. M. Steffen, and R. M. Wheeler, Nucl. Data Tables **11**, 351 (1973).
[5] M. P. Waring, E. S. Paul, C. W. Beausang, R. M. Clark, R. A. Cunningham, T. Davinson, S. A. Forbes, D. B. Fossan, S. J. Gale, A. Gizon, K. Hauschild, I. M. Hibbert, A. N. James, P. M. Jones, M. J. Joyce, D. R. LaFosse, R. D. Page, I. Ragnarsson, H. Schnare, P. J. Sellin, J. Simpson, P. Vaska, R. Wadsworth, and P. J. Woods, Phys. Rev. C **51**, 2427 (1995).
[6] G. J. Lane, D. B. Fossan, I. Thorslund, E. S. Paul, J. Simpson, D. J. Blumenthal, C. N. Davids, C. J. Lister, and D. Seweryniak, Phys. Rev. C **55**, 1559 (1997).
[7] A. J. Boston, E. S. Paul, C. J. Chiara, M. Devlin, D. B. Fossan, S. J. Freeman, D. R. LaFosse, G. J. Lane, M. Leddy, I. Y. Lee, A. O. Macchiavelli, P. J. Nolan, D. G. Sarantites, J. M. Sears, A. T. Semple, J. F. Smith, and K. Starosta (unpublished).
[8] Zs. Dombradi, B. M. Nyako, G. E. Perez, A. Algora, C. Fahlander, D. Seweryniak, J. Nyberg, A. Atac, B. Cederwall, A. Johnson, A. Kerek, J. Kownacki, L. O. Norlin, R. Wyss, E. Adamides, E. Ideguchi, R. Julin, S. Juutinen, W. Karczmarczyk, S. Mitarai, M. Piiparinen, R. Schubart, G. Sletten, S. Tormanen, and A. Virtanen, Phys. Rev. C **51**, 2394 (1995).
[9] G. de Angelis, C. Fahlander, A. Gadea, E. Farnea, D. Bazzacco, N. Belcari, N. Blasi, P. G. Bizzeti, A. Bizzeti-Sona, D. de Acuna, M. de Poli, H. Grawe, A. Johnson, G. Lo Bianco, S. Lunardi, D. R. Napoli, J. Nyberg, P. Pavan, J. Persson, C. Rossi Alvarez, D. Rudolph, R. Schubart, P. Spolaore, R. Wyss, and F. Xu, Phys. Lett. B **437**, 236 (1998).
[10] D. D. Bogdanov, S. Darotsi, V. A. Karnaukhov, L. A. Petrov, and G. M. Ter-Akopyan, Yad. Fiz. **6**, 893 (1967) [Sov. J. Nucl. Phys. **6**, 650 (1968)].
[11] J. Blachot, Nucl. Data Sheets **81**, 753 (1997).
[12] J. Blachot, Nucl. Data Sheets **83**, 647 (1998).
[13] S. Vajda, A. Iordachescu, E. A. Ivanov, and G. Pascovici, Phys. Lett. **42B**, 54 (1972).
[14] M. Hass, H. H. Bertschat, C. Broude, E. Dafni, F. D. Davidovsky, G. Goldring, and P. M. S. Lesser, Nucl. Phys. **A410**, 317 (1983).
[15] Ch. Droste, D. Chlebowska, J. Dobaczewski, F. Dönau, A. Kerek, G. Leander, J. Srebrny, and W. Waluś, Nucl. Phys. **A341**, 98 (1980); F. Dönau and U. Hagemann, Z. Phys. A **293**, 31 (1979) and references therein.
[16] H. Dias and L. Losano, Phys. Rev. C **50**, 1377 (1994), and references therein.
[17] K. Starosta, Ch. Droste, T. Morek, J. Srebrny, D. B. Fossan, S. Gundel, J. M. Sears, I. Thorslund, P. Vaska, M. P. Waring, S. G. Rohoziński, W. Satuła, U. Garg, S. Naguleswaran, and J. C. Walpe, Phys. Rev. C **55**, 2794 (1997).
[18] T. Morek, K. Starosta, Ch. Droste, D. B. Fossan, G. Lane, J. M. Sears, J. F. Smith, and P. Vaska, Eur. Phys. J. A **3**, 99 (1998).
[19] A. Bohr and B. Mottelsson, *Nuclear Structure* (Benjamin, New York, 1975), Vol. 2.
[20] J. M. Eisenberg and W. Greiner, *Nuclear Theory* (North-Holland, Amsterdam, 1987), Vol. 1.
[21] S. Raman, C. H. Malarkey, W. T. Milner, C. W. Nester, Jr., and P. H. Stelson, At. Data Nucl. Data Tables **42**, 1 (1989).
[22] E. S. Paul, H. R. Andrews, T. E. Drake, J. DeGraaf, V. P. Janzen, S. Pilotte, D. C. Radford, and D. Ward, Phys. Rev. C **50**, R534 (1994).
[23] S. Ćwiok, J. Dudek, W. Nazarewicz, J. Skalski, and T. Werner, Comput. Phys. Commun. **46**, 379 (1987).
[24] D. R. Bes and R. A. Sorensen, in *Advances in Nuclear Physics*, edited by M. Baranger and E. Vogt (Plenum Press, New York, 1969), Vol. 2, p. 129.
[25] A. Arima, Nucl. Phys. **A354**, 19c (1981).
[26] D. R. LaFosse *et al.* (unpublished).
[27] R. Devi and S. K. Khosa, Z. Phys. A **354**, 45 (1996).
[28] J. Rikovska, N. J. Stone, P. M. Walker, and W. B. Walters, Nucl. Phys. **A505**, 145 (1989).
[29] R. Wyss, J. Nyberg, A. Johnson, R. Bengtsson, and W. Nazarewicz, Phys. Lett. B **215**, 211 (1988).
[30] L. Kaubler, H. Prade, J. Reif, R. Schwengner, G. Winter, H. Grawe, J. Heese, H. Kluge, K.-H. Maier, R. Schubart, and K.-M. Spohr, Z. Phys. A **351**, 123 (1995); Phys. Scr. **T56**, 266 (1995).
[31] E. S. Paul, C. W. Beausang, S. A. Forbes, S. J. Gale, A. N. James, P. M. Jones, M. J. Joyce, H. R. Andrews, V. P. Janzen, D. C. Radford, D. Ward, R. M. Clark, K. Hauschild, I. M. Hibbert, R. Wadsworth, R. A. Cunningham, J. Simpson, T. Davinson, R. D. Page, P. J. Sellin, P. J. Woods, D. B. Fossan, D. R. LaFosse, H. Schnare, M. P. Waring, A. Gizon, J. Gizon, T. E. Drake, J. DeGraaf, and S. Pilotte, Phys. Rev. C **50**, 698 (1994).

[32] J. Skalski, Phys. Lett. B **238**, 6 (1990); P. A. Butler and W. Nazarewicz, Rev. Mod. Phys. **68**, 349 (1996).

[33] G. J. Lane, D. B. Fossan, J. M. Sears, J. F. Smith, J. A. Cameron, R. M. Clark, I. M. Hibbert, V. P. Janzen, R. Krücken, I. Y. Lee, A. O. Macchiavelli, C. M. Parry, and R. Wadsworth, Phys. Rev. C **57**, R1022 (1998).

[34] J. J. Van Ruyven, W. H. A. Hesselink, J. Akkermans, P. Van Nes, and H. Verheul, Nucl. Phys. **A380**, 125 (1982).

[35] A. I. Vdovin, Ch. Stoyanov, and W. Andrejtscheff, Nucl. Phys. **A440**, 437 (1985).

[36] M. Fukuda, Y. Nagai, T. Irie, and H. Ejiri, Nucl. Phys. **A470**, 1 (1987).